PHYSICAL REVIEW B, VOLUME 63, 081403(R)

Liquid-crystal phases of capped carbon nanotubes

Andrés M. Somoza,[1] Celeste Sagui,[2] and Christopher Roland[2]
[1]*Departamento de Física, Universidad de Murcia, E-30071, Murcia, Spain*
[2]*Department of Physics, North Carolina State University, Raleigh, North Carolina 27695*
(Received 28 July 2000; published 1 February 2001)

With continuum-based density-functional theory, we have analyzed the liquid-crystal phases of finite-sized capped carbon nanotubes as a function of nanotube length and diameter for (i) the case when the nanotubes interact via the fully attractive van der Waals force; and (ii) when such interactions are screened out and the force is hard-core repulsive only. In the case of the former, we find that the columnar phase preempts all other phases at any reasonable temperature. This result is consistent with the formation of nanotube ropes during the high-temperature growth processes in laser vaporization and carbon arc experiments.

DOI: 10.1103/PhysRevB.63.081403 PACS number(s): 71.10.Hf, 71.20.Tx, 73.21.−b

Carbon nanotubes are perhaps one of the most interesting of the new materials to emerge during the past decade. Because of their size, symmetry, and outstanding mechanical properties, carbon nanotubes may well provide a fundamental and natural structural component for the emerging field of nanotechnology.[1] There is also considerable excitement associated with the electronic properties of carbon nanotubes. Depending on their helicity, single-wall nanotubes are either metallic or semiconducting, and therefore have the potential of forming the basis of a future all-carbon, nanotube-based microelectronics.[2] It is also clear that *finite-sized* carbon nanotubes are variable-length rods, which by virtue of their shape and size can act as liquid crystals.[3] To examine the possibility of nanotubes forming *tailored* liquid crystals for application purposes, we investigated the phase diagrams of capped nanotubes as a function of nanotube length and diameter in two limits: in the presence of the attractive van der Waals forces, and in the hard-rod limit characteristic of nanotubes in which such interactions are completely screened. Our results show that when attractive interactions are present, the columnar phase preempts all others at room temperatures.

Experimentally, capped finite-sized nanotubes are produced as follows. Carbon nanotubes are most commonly formed in either an arc discharge,[4] or via laser vaporization.[5] In the presence of small amounts of metal catalysts, *single-wall* nanotubes are the dominant product, while *multiwalled* tubes form in their absence. Typically, single-wall nanotubes are formed as a deposit consisting of weblike bundles of nanotube ropes along with other fullerene and amorphous carbon products. The deposit is readily purified to form a free-standing mat of tangled nanotube ropes, termed ''bucky paper.'' Each of the constituent nanotube ropes typically consists of several hundreds of nanotubes whose cross sections form, more or less, a hexagonal lattice. The nanotubes may be cut and separated via prolonged sonication in a 3:1 mixture of sulfuric and nitric acid at 40 °C.[6] The resulting ''fullerene pipes'' have an average length of about 280 nm. This length may be further reduced to about 150 nm, or lower, by heating the tubes in the same acid mixture with only gentle stirring. The cut nanotubes may then be sorted according to their length via field-flow fractionation. While this procedure forms open nanotube pipes, these may readily be closed by true hemifullerene end-caps simply by annealing the pipes in vacuum in the 1000−1200 °C temperature range.[6]

To calculate the phase diagram of capped nanotubes, we used density-functional theory[7] within the context of a generalized van der Waals model,[8] as in other liquid-crystal calculations. Since these theoretical techniques are well known, our description of the method will be brief and restricted to details directly pertaining to the calculations. In a generalized van der Waals model, the free energy F as a functional of the density ρ is split into two parts: a term for the hard-core density-functional F_{HC}, and a term for the longer-ranged attractive interactions which can be treated in the context of mean-field theory, so that in general

$$F[\rho(\vec{r},\vec{\omega})] = F_{HC}[\rho(\vec{r},\vec{\omega})] + \frac{1}{2}\int d\vec{r}_1 \int d\vec{r}_2 \int d\vec{\omega}_1 \times \int d\vec{\omega}_2 \rho(\vec{r}_1,\vec{\omega}_1)\rho(\vec{r}_2,\vec{\omega}_2) \times V_{eff}(\vec{r}_1-\vec{r}_2,\vec{\omega}_1,\vec{\omega}_2), \quad (1)$$

where $\rho(\vec{r},\vec{\omega})$ is the probability of finding a nanotube center at $\vec{r}$ with its *three-dimensional* orientation in direction $\vec{\omega}$; and V_{eff} the effective attractive potential between the different nanotubes. We separate the pair potential in attractive and repulsive contributions using the Barker-Henderson method,[8] i.e., V_{eff} is equal to the full pair potential when this is negative and it is zero otherwise. To calculate the effective potential between two capped nanotubes, which are assumed to be stiff and oriented as shown in Fig. 1, we use a continuous version of the Girifalco-Lad[9] potential, whose parameters are fitted to reproduce the structural properties of graphite. The potential models the van der Waals interaction between carbon atoms on two different graphene sheets as $V_{CC}(d) = C_{12}/d^{12} - C_6/d^6$, where d is the distance between carbon atoms, and the other parameters are $C_{12} = 24\,800$ eV (Å^{12}) and $C_6 = 20$ eV. (Å^6) An effective potential cutoff of 16.4 Å is assumed. To simplify the calculations, this potential was spread uniformly over the surface of the nanotubes with a proper atomic density so that

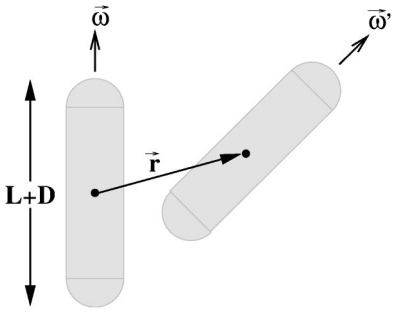

FIG. 1. Schematic of geometrical setup for the calculation of V_{eff}. Here $\vec{r}$ denotes the vector joining the centers of two nanotubes of length $L+D$, where D is the nanotube diameter. The axis of the nanotubes point in the $\vec{\omega}$ and $\vec{\omega}'$ directions, as shown.

$$V_{eff}(\vec{r},\vec{\omega},\vec{\omega}')=\int_{S_1} d\vec{S}_1 \int_{S_2} d\vec{S}_2 V_{CC}(\vec{S}_1-\vec{S}_2)\sigma^2,$$

where $\vec{S}_1$ and $\vec{S}_2$ denote surface elements on two different nanotubes, and $\sigma=0.383$ Å^{-2}. The continuum-based results for V_{eff} were also compared to the corresponding discrete results, which were obtained by modeling the carbon nanotubes with standard classical potentials[10] with V_{CC} superimposed to model the internanotube van der Waals interaction. The two results are in excellent agreement, and differ by less than 10% so that the final phase diagrams would be virtually identical. We also note that this continuum version of the pair potential has previously been also used to study vibrational properties of carbon nanotube bundles.[11]

Finally, we use a reliable hard-core free energy function F_{HC} from the liquid-crystal literature,[12] which effectively recovers the Onsager limit $L\to\infty$ for the isotropic-nematic transition and, in the limit of hard-spheres, $L\to 0$, it reproduces a well tested density functional.[13] This free-energy functional has previously been tested for parallel spherocylinders,[14] freely rotating spherocylinders,[15] and the Gay-Berne model.[16] Having defined F, one can then numerically calculate the chemical potential $\mu=\delta F[\rho]/\delta\rho$ at a given temperature T and calculate phase diagrams by standard statistical methods.

The main results of our calculations are shown in Fig. 2, which displays temperature (T) versus packing fraction (η) phase diagrams for capped nanotubes of different lengths and diameters subject to the full van der Waals interaction. Top panels show phase diagrams for the relatively narrow 6.8 Å nanotubes, while the bottom panels display results for wider 13.5 Å diameter tubes. Similarly, left to right panels show results for increasing nanotube lengths of $L+D=50$, 100, and 200 nm, respectively. In Fig. 2, the shaded gray region denotes the vapor-liquid- or isotropic-nematic coexistence regions, while the dashed line corresponds to an approximation to the nematic-columnar spinodal curve as described below. The solid vertical line marks the isotropic-nematic coexistence region for nanotubes with *no attractive interactions* present in the system, i.e., the effects of hard core interactions between nanotubes only.

What does this figure tell us? First, it is clear that the phase diagrams are complex, displaying features that are

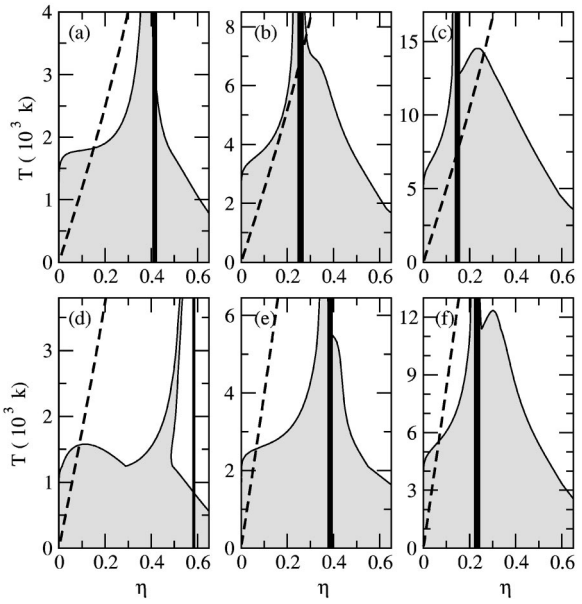

FIG. 2. Calculated phase diagrams for nanotubes of length L and diameter D as a function of temperature T and packing fraction η. Parameters for the capped nanotubes are (a) $L+D=50$ nm, $D=6.8$ Å; (b) $L+D=100$ nm, $D=6.8$ Å; (c) $L+D=200$ nm, $D=6.8$ Å; (d) $L+D=50$ nm, $D=13.5$ Å; (e) $L+D=100$ nm, $D=13.5$ Å; (f) $L+D=200$ nm, $D=13.5$ Å. The shaded grey region denotes the isotropic-nematic coexistence region and the dashed line the nematic-columnar spinodal. The thick solid line marks the isotropic-nematic coexistence region in the absence of any *attractive interactions*, i.e., it represents the hard-core limit that is temperature independent.

similar to other work on liquid crystals. For instance Fig. 2(a) shows that there is vapor-liquid-nematic triple point, while Fig. 2(c) shows an isotropic-nematic-nematic triple point. Unfortunately, all of these interesting features occur at unreasonably high temperatures of several thousand degrees Kelvin, which are temperatures where one cannot expect the nanotubes to be stable. Hence, many of these features are simply not relevant when discussing the liquid-crystal phases of carbon nanotubes. Physically, this fact is a simple reflection of the very strong interaction between nanotubes, which may be quite large because of the huge number of atoms that are involved.

Figure 2 also marks the stability edge of the nematic phase with respect to phases with positional order: assuming perfect nematic order, we have calculated the structure factor $S(T,\eta,\vec{k})$ which in turn allows one to calculate the spinodal lines by probing for points of T and η where $S(\vec{k})$ diverges. We find that the carbon nanotube system is dominated by the nematic-columnar spinodal, which rises steeply from very small values of η to very high temperatures.[17] Since most of the phase diagram lies to the right of this line, one can expect that the columnar phase will preempt any sort of nematic or smectic phases, except perhaps for very small values of η, which lie to the left of this line. This area to the left of the columnar-nematic spinodal decreases sharply with increasing nanotube length, and increases only weakly as the nanotube diameter is enlarged. This dominance of the columnar phase

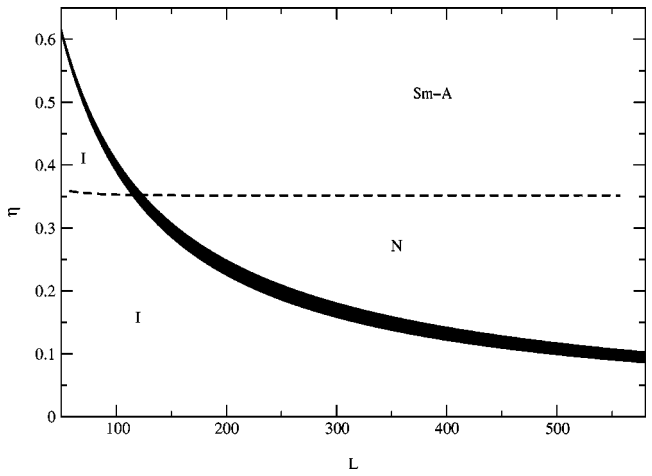

FIG. 3. Isotropic-nematic coexistence region as a function of nanotube lengths for tubes of diameter $D=13.5$ Å in the hard-core limit (i.e., no attractive van der Waals interaction) separating the isotropic (I) and nematic (N) phases is shown by the solid line. The dashed line marks the separation between the nematic and smectic-A (Sm-A) phases.

over the smectic phases is another manifestation of the strong attractive interaction between nanotubes, and is different from the cases previously considered. In general, thermotropic liquid crystals and simulation of hard-core molecules[18,19] show that the smectic phases are associated with prolate molecules and the columnar phases with the oblate ones. These systems, however, are all dominated by the repulsive interaction terms, which is opposite from the nanotube case where the attractive interactions lead to a reversal of this trend. Experimentally, the domination of the columnar phase is completely consistent with the structure of the nanotube ropes, which internally consists of very long nanotubes in the columnar phase. The persistence of the columnar phase at very high temperatures also explains why no other structures have consistently been observed in the tangled webs of quenched nanotubes.

While the columnar phase will dominate when there are van der Waals interactions between the nanotubes, different phases are possible in the absence of any attractive interactions, when the system is dominated by its hard-core repulsion only. Such a situation could arise, for instance, for nanotubes dispersed in low-molecular weight organic liquids which could effectively screen out the van der Waals interactions between the tubes.[6] In Fig. 2, the thick vertical black line marks the isotropic-nematic coexistence region in this limit. As expected, this region is completely independent of temperature and essentially coincides with the (very) high-temperature limit of isotropic-nematic phase diagram with van der Waals interactions present. Note also that this coexistence region shifts from large to small values of η as the nanotube length increases, and that the coexistence region enlarges somewhat. This is a reflection of the change in the aspect ratio as the length of the nanotubes increases: as η decreases the system becomes more compressible and allows for a larger change $\Delta\eta$ at the transition. Figure 3 shows a more detailed phase diagram for nanotubes in this limit as a function of length and η: the smectic-A (sm-A) phase is separated from the nematic phase by the dashed line ($\eta \approx 0.36$), while the thick line separated the isotropic and nematic phases. These results are completely consistent with previous work on liquid-crystal phases,[15] where a different approximation was used to calculate the nematic-smectic phase transition.

To summarize, we have calculated the phase diagrams of capped carbon nanotubes both in the presence and absence of van der Waals interactions using density-functional theory within a generalized van der Waals model. In the presence of full van der Waals interaction between the nanotubes, the calculations show that the *columnar phase* preempts all the other phases to very high temperatures. This result is consistent with the formation of nanotube ropes during the high-temperature growth, as seen in both laser vaporization and carbon arc experiments. In the absence of such interactions, for instance in the presence of low molecular-weight organic solvents which screen out the van der Waals interactions, both nematic and smectic-A phases should be obtainable at relatively high packing fractions.

We gratefully acknowledge scientific discussions with Professor J. Bernholc and Professor A. Rubio. For financial support, we thank the following agencies: ONR N00014-98-1-0597 and NASA NAG8-1479 (C.R.); NSF POWRE-9870464 (C.S.); and PB96-1120 DGICyT, Spain (A.M.S.). We also thank the North Carolina Supercomputing Center (NCSC) for extensive computer support.

[1] R.F. Service, Science **281**, 940 (1998).

[2] See, for example, M.S. Dresselhaus, G. Dresselhaus, and P.C. Eklund, *Science of Fullerenes and Carbon Nanotubes* (Academic, San Diego, 1996); J. Bernholc, C. Roland, and B.I. Yakobson, Curr. Opin. Solid State Mater. Sci. **2**, 706 (1997).

[3] For reviews on liquid crystal, see for example, P.G. de Gennes and J. Prost, *The Physics of Liquid Crystals*, 2nd ed. (Oxford University Press, 1995); S. Chandrasekhar, *Liquid Crystals*, 2nd ed. (Cambridge University Press, Cambridge, 1992).

[4] S. Iijima, Nature (London) **354**, 56 (1991); T.W. Ebbessen and P.M. Ajayan, *ibid.* **358**, 220 (1992); D.S. Bethune, C.H. Kiang, M.S. de Vries, G. Gorman, R. Savoy, J. Vascus, and R. Beyers, *ibid.* **363**, 605 (1993).

[5] D.T. Colbert, J. Zhang, S.M. McClure, P. Nikolaev, Z. Chen, J.H. Hafner, D.W. Owens, P.G. Kotula, C.B. Carter, J.H. Weaver, A.G. Rinzler, and R.E. Smalley, Science **266**, 1218 (1994).

[6] J. Liu, A.G. Rinzler, H. Dai, J.H. Hafner, R. Kelley Bradley, P.J. Boul, A. Lu, T. Iverson, K. Shelimov, C.B. Huffman, F. Rodriques-Macias, Y-S Shon, T.R. Lee, D.T. Colbert, and R.E. Smalley, Science **280**, 1253 (1998).

[7] See, for example, R. Evans, Adv. Phys. **28**, 143 (1979).

[8] See, for example, J.-P. Hansen and I.R. McDonald, *Theory of Simple Liquids* (Academic Press, New York, 1990).

[9] L.A. Girifalco and R.A. Lad, J. Chem. Phys. **25**, 693 (1956).

[10] J. Tersoff, Phys. Rev. Lett. **56**, 632 (1986); **61**, 2879 (1988); Phys. Rev. B **37**, 6991 (1988); D.W. Brenner, *ibid.* **42**, 9458 (1990).

[11] L. Henrard, E. Hernández, P. Bernier, and A. Rubio, Phys. Rev. B **60**, R8521 (1999).

[12] A.M. Somoza and P. Tarazona, Phys. Rev. Lett. **61**, 2566 (1988); J. Chem. Phys. **91**, 2461 (1989).

[13] P. Tarazona, Phys. Rev. A **31**, 2672 (1985).

[14] A.M. Somoza and P. Tarazona, Phys. Rev. A **40**, 4161 (1989).

[15] A.M. Somoza and P. Tarazona, Phys. Rev. A **41**, 965 (1990); **40**, 6069 (1989).

[16] E. Velasco and L. Mederos, J. Chem. Phys. **109**, 2361 (1998); V.V. Ginzburg, M.A. Glaser, and N.A. Clark, Liq. Cryst. **21**, 264 (1997).

[17] On a technical note, it may be argued that our procedure slightly overestimates the stability of the columnar phase for two reasons: the use of the free-energy functional and the assumption of parallel nanotubes both underestimate the short-range correlations of nematic phase somewhat. However, these effects should be small and do not effect our basic results in any significant way.

[18] P.G. Bolhuis, A. Stroobants, D. Frenkel, and H.N.W. Lekkerkerker, J. Chem. Phys. **107**, 1551 (1997).

[19] H. Graf and H. Lowen, Phys. Rev. E **59**, 1932 (1999).